ACS Macro Letters

Letter

pubs.acs.org/macroletters

Organic–Inorganic Hybrid Nanoparticles via Photoinduced Micellation and Siloxane Core Cross-Linking of Stimuli-Responsive Copolymers

Christian Anger,[⊥] Frank Deubel,[⊥] Stephan Salzinger,[⊥] Jürgen Stohrer,[†] Tobias Halbach,[†] Rainer Jordan,[§] Jonathan G. C. Veinot,[‖] and Bernhard Rieger*

Institut für Siliciumchemie, TU München Lichtenbergstraße 4, 85748 Garching, Germany

Supporting Information

ABSTRACT: Photoacid-induced siloxane cross-linking of stimuli-responsive copolymer micelles allows the synthesis of well-defined organic–inorganic hybrid nanoparticles. Two conceptually different synthetic approaches are presented, both via photoinduced cross-linking of poly(4-hydroxystyrene-*block*-styrene) micelles and via *one-pot* photoacid-catalyzed micelle formation and siloxane cross-linking of poly(4-*tert*-butoxystyrene-*block*-styrene). The *multistep* synthetic route showed intermicellar cross-linking leading to agglomerates. In contrast to this, the formation of the nanoparticles via the one-pot synthesis yielded well-defined structures. The use of different siloxane cross-linking agents and their effects on the properties of the cross-linked micellar structures have been evaluated. Scanning electron microscopy and differential scanning calorimetry indicate rigid core cross-linked nanoparticles. Their size, molar mass, and swelling behavior were analyzed by dynamic and static light scattering. Cyclic siloxane cross-linking agents lead to residual C═C double bonds within the nanoparticle core that allow postsynthetic modification by, e.g., thiol–ene click reactions.

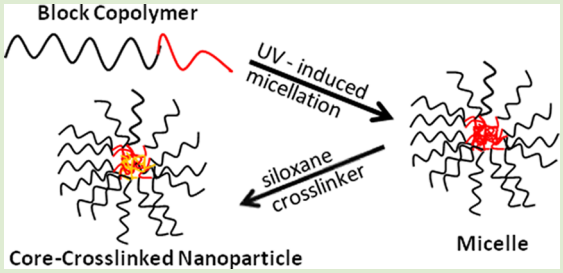

Hybrid organic–inorganic materials are the focus of substantial research interest because of the potential of synergistic effects that could arise by combining these complementary components giving rise to promising new material properties. These substances can be obtained via a wide range of synthetic strategies. Among these, core cross-linking of micelles represents a straightforward approach to yield well-defined organic–inorganic hybrid structures. Using the self-assembly of stimuli-responsive block copolymers, this synthetic route can be externally triggered. This class of polymers has attracted much attention and has found wide-ranging applications including sensors,[1−3] drug delivery,[4−6] and data storage.[7] Micelle self-assembly can be induced using different stimuli, such as changes in pH,[8] temperature,[9,10] or pressure,[11,12] exposure to light,[13−15] redox reactions,[16−18] or a combination thereof.[19] Light is a particularly interesting "trigger" that can induce reversible[19−26] and irreversible[13,27−31] structural changes. Recently, Yoshida et al.[32] reported micelle formation via photochemical deprotection of poly(4-*tert*-butoxystyrene-*block*-styrene) (P4^{t}BS-*b*-PS) in the presence of a photoacid generator (PAG).

In this work, we describe the preparation of micelles and their subsequent covalent core cross-linking by photoinduced condensation of pendant hydroxy groups with siloxanes to produce hybrid organic–inorganic nanoparticles (see Scheme 1). We investigate two complementary pathways for photoinduced cross-linking of polymeric micelle cores: Our first approach (Scheme 1A) employs a *multistep* procedure with no fewer than three steps: (i) P4^{t}BS-*b*-PS is hydrolyzed by hydrochloric acid in THF to yield poly(4-hydroxystyrene-*block*-styrene) (P4HS-*b*-PS). (ii) The purified polymer micelles of P4HS-*b*-PS are immediately formed in dichloromethane. (iii)

Scheme 1. Formation of Hybrid Organic–Inorganic Nanoparticles from a Stimuli-Responsive Block Copolymer by Core Cross-Linking of Micelles by a Multistep (A) or One-Step Synthetic Route (B)

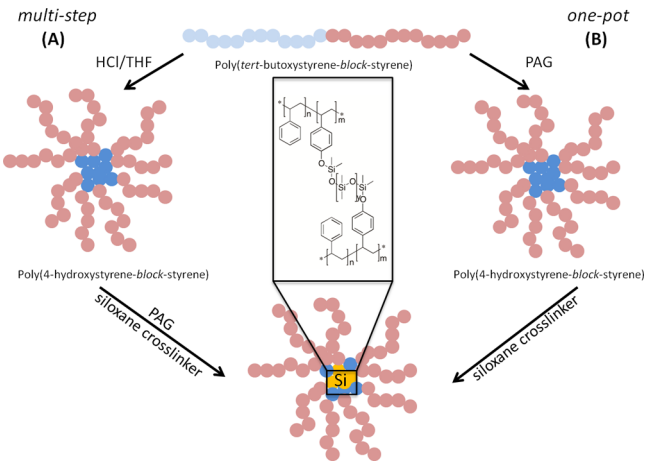

Received: December 14, 2012
Accepted: January 8, 2013
Published: January 15, 2013

The core is cross-linked via photoacid-catalyzed condensation reaction using diphenyliodonium hexafluorophosphate (DHP). By the use of different cross-linkers, the chemical properties of the polysiloxane in the core can be tailored. The second approach is a "*one-pot*", two-step synthesis involving block copolymer hydrolysis, micelle formation, and PAG-mediated core cross-linking with alkoxysilanes (Scheme 1B).

Herein, we report the influence of different cross-linking agents and synthetic methodologies. The presented hybrid organic−inorganic nanoparticles were characterized in detail using dynamic and static light scattering, gel permeation chromatography multiangle light scattering (GPC-MALS), scanning electron microscopy, and NMR spectroscopy. The resulting material might be of particular interest for numerous applications including drug delivery, diagnostic imaging, or as precursors for nanoelectronic devices.[33−37]

For the present study, the preparation of P4^{t}BS-*b*-PS by nitroxide-mediated controlled radical polymerization with 2,2,6,6-tetramethylpiperidinyl-1-oxyl was achieved using literature procedures (Supporting Information, Scheme S2).[32] The P4^{t}BS block showed a narrow polydispersity (i.e., PDI = 1.15) and a weight-average molecular weight of 18 500 g/mol. The subsequent block copolymerization with styrene resulted in P4^{t}BS-*b*-PS with an overall dispersity of 1.6 (M_w = 223 500 g/mol; Supporting Information, Table S1).

For the PAG-mediated cross-linking of the P4HS-*b*-PS micellar core, we chose to use cross-linking agents possessing tertiary alkoxy substituents pendant on the silicon center. This structural feature is crucial to the eventual cross-linking of the micelles under the presented conditions because these tertiary alkoxy substituents can be transformed to a silanol group via a photoacid-induced alkyl cleavage. The resulting silanol groups can subsequently undergo an acid-catalyzed polycondensation reaction within the polymer micelle.

Two cross-linking agents expected to satisfy these requirements were synthesized (Supporting Information, Scheme S1). Di-*tert*-butoxydimethylsilane (DBDMS) was chosen because it is a small cross-linking reagent that is expected to readily diffuse into polymer micelles. In contrast, 2,2,8,8-tetramethyl-1,7-dioxa-6-silaspiro[5.5]undecane (OSSC-6) is comparatively large, and it reacts via a ring-opening mechanism without the release of volatile low molar mass compounds. Furthermore, cross-linking of the sterically more demanding OSSC-6 leads to formation of double bonds within the micelle core network that may offer a platform for selective core functionalization.[38] This aspect of these materials is the subject of ongoing studies in our laboratory.

DBDMS was synthesized from dimethyldichlorosilane via nucleophilic substitution with *tert*-butanol (Supporting Information, Scheme S1). To avoid acid-catalyzed hydrolysis by the HCl byproduct, 1-methylimidazole was added as a scavenger. OSSC-6 was synthesized via tris(pentafluorophenyl)borane-catalyzed double intramolecular hydrosilylation of bis((2-methylpent-4-en-2-yl)oxy)silane, which was prepared using a synthetic scheme analogous to that used for DBDMS.

Pathways toward photoinduced internal cross-linking of polymer micelles with alkoxysilanes are summarized in Scheme 2. Detailed experimental procedures are provided in the Supporting Information. Micelles were characterized via DLS, SLS, SEM, NMR, and DSC before and after cross-linking.

Dynamic light scattering was performed at different stages of micelle formation. Before cross-linking, the average hydrodynamic radius of the P4HS-*b*-PS micelles obtained by prior *tert*-butyl cleavage was found to be 195 nm. This is approximately 20 nm larger than the hydrodynamic radii determined of micelles formed in the one-pot route (175 nm, in dichloromethane, Figures 1 and 2).

Scheme 2. (a) Micelle Formation by HCl Treatment and Successive Alkoxysilane Cross-Linking and (b) One-Pot Photoacid-Catalyzed Micelle Formation and Alkoxysilane Cross-Linking

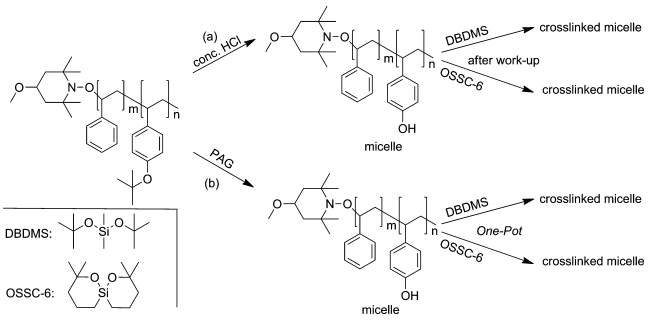

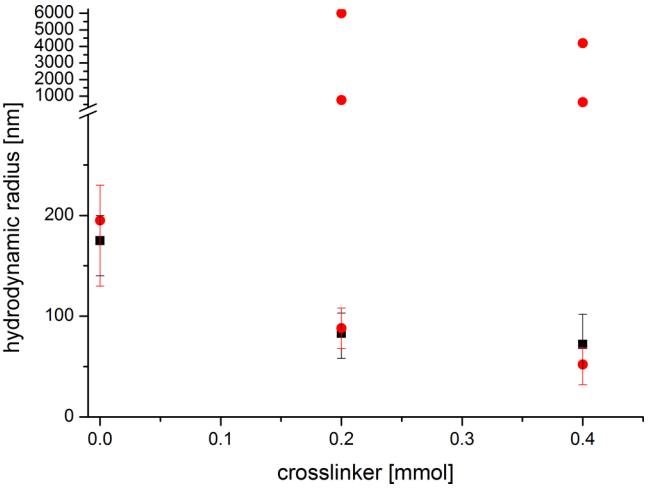

Figure 1. DLS results in dichloromethane for successive micelle formation via multistep (red circles) and one-pot cross-linking (black squares) using di-*tert*-butoxydimethylsilane. The dispersity of the micelles and nanoparticles is given by the error bars.

Addition of 0.2 mmol of the DBDMS cross-linker to purified P4HS-*b*-PS decreases the hydrodynamic radius of the micelles from 195 to 89 nm (54% shrinkage; Figure 1). Addition of larger quantities of DBDMS (i.e., 0.4 mmol) causes a larger decrease in the hydrodynamic radius (i.e., r_h = 53 nm; 73% shrinkage). This behavior is attributed to different swelling responses of the non-cross-linked and cross-linked particles. For the former, the hydrophilic core shows characteristic swelling in dichloromethane, and this swelling is minimized by core cross-linking, leading to particle shrinkage. Unfortunately, a significant disadvantage of the present multistep synthetic protocol arises from *inter*micellar cross-linking reactions. This deleterious reaction is evidenced by the appearance of large aggregates with average sizes between 600 and 5200 nm in SEM imaging and DLS (i.e., 50−34 wt % for 0.2 and 0.4 mmol of cross-linker, respectively). The determination of mass fractions of nanoparticles and aggregates by DLS cannot be

dx.doi.org/10.1021/mz3006439 | *ACS Macro Lett.* 2013, 2, 121−124

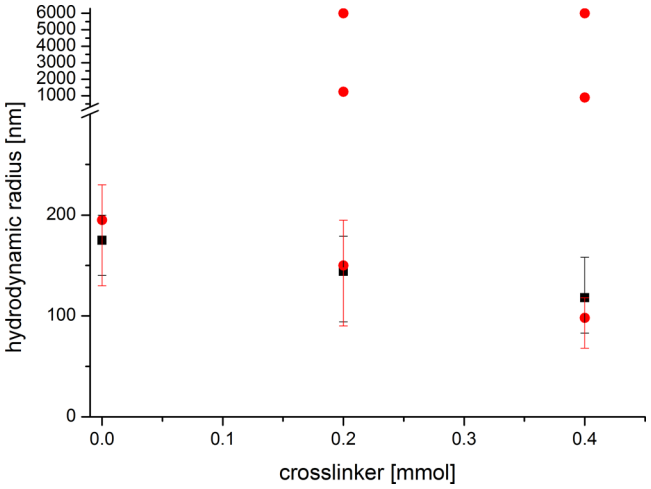

Figure 2. DLS results in dichloromethane for micelle formation via multistep cross-linking (red circles) and one-pot cross-linking (black squares) using 2,2,8,8-tetramethyl-1,7-dioxa-6-silaspiro[5.5]undecane. The dispersity of the micelles and nanoparticles is given by the error bars.

considered quantitative because the number of aggregates measured is not statistically significant.

In contrast, for the one-pot synthesis, for which micelles are combined with 0.2 mmol of DBDMS and irradiated for two hours, the DLS measurement showed a hydrodynamic radius of the obtained particles of 84 nm. Particle dimension decreased to 72 nm when 0.4 mmol of alkoxysilane was used. These observations (i.e., 52% and 59% shrinkage, respectively) are consistent with the same cross-linking processes occurring for both synthetic routes; however, the multistep procedure yields products with significant quantities of larger diameter impurities that could limit or even preclude future applications.

When identical cross-linking procedures are employed with the more sterically demanding OSSC-6 cross-linker, a substantially less pronounced micelle shrinkage is observed. Specifically, we observe 23−44% for the multistep synthesis versus 20−32% for the one-pot method, for 0.2 and 0.4 mmol of cross-linker, respectively (Figure 2). In contrast, the aggregate particle size formed during the multistep synthesis is only slightly larger (1000 and 5200 nm) than for the cases where cross-linking was achieved using DBDMS. In addition, for OSSC-6 cross-linked samples, the aggregate mass fraction for the multistep synthesis procedure shows an increase of 27−37 wt % for 0.2 and 0.4 mmol of siloxane compound. Recall that because of sampling limitations these data only provide qualitative information (vide supra).

To better understand the origin of the external cross-linking, the multistep synthesis protocol was altered, and further cross-linking experiments were conducted. DHP was added to the purified P4HS-*b*-PS, and the resulting mixture was irradiated for 60 min. The hydrodynamic micelle radius was not affected, indicating the present micelles are stable in the presence of a PAG. After addition of the alkoxysilane compound, still, formation of large aggregates was observed. In this context, we conclude even prolonged equilibration does not facilitate complete PAG diffusion into the micelle interiors. Consequently, irradiation of these mixtures leads to the formation of polysiloxanes outside the micelles and external micelle cross-linking. Because this side reaction is not observed for the present one-pot synthesis, we conclude that the polarity of the PAG leads to effective encapsulation in the micelles during their formation.

The impact of cross-linking on particle morphology was evaluated by scanning electron microscopy (SEM), revealing a characteristic "doughnut"-like structure, formed during drying-induced flattening for non-cross-linked particles (Figure 3a).

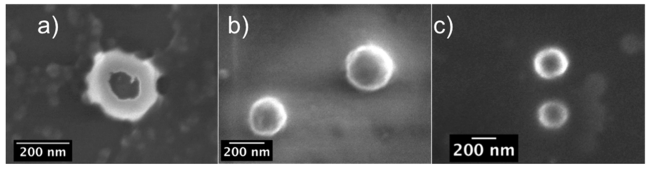

Figure 3. Representative secondary electron SEM micrographs of (a) a non-cross-linked micelle and nanoparticles obtained from the one-pot cross-linking procedure using (b) 0.2 mmol and (c) 0.4 mmol of OSSC-6.

After cross-linking with OSSC-6, only negligible flattening occurs, and the integrity of the three-dimensional structures is maintained (Figure 3b and c). Because DLS provides a measure of hydrodynamic dimensions and SEM is a direct measure of dried particles, the observed differences in absolute measurements are not unexpected. Still, an obvious trend of particle shrinkage for increased internal cross-linking is evident.

Consistent with DLS results noted for the multistep synthesis protocol, individual nanoparticles and large nanoparticle aggregates resulting from external cross-linking micelles are observed (Figure 4). SEM analysis of nanoparticles formed with the one-pot synthesis approach showed no such intermicellar cross-linking.

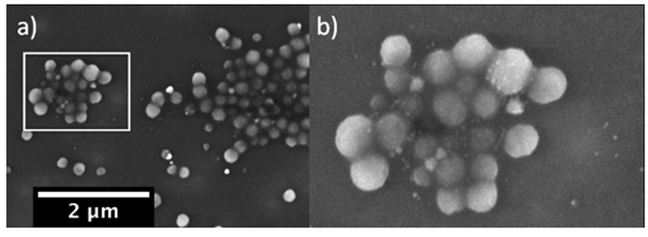

Figure 4. Representative secondary electron scanning electron micrographs showing large aggregates formed by external cross-linking for the multistep synthesis protocol.

Differential scanning calorimetry (DSC) indicates covalent cross-linking of the present micelles leading to a significant change of the material thermal properties. P4HS-*b*-PS micelles show a T_g of 103 °C, independent of the synthesis procedure (Supporting Information, Table S2: entry 2). Addition of DBDMS leads to a minor decrease (to 97−101 °C) and broadening of the glass transition (Supporting Information, Table S2: entries 3 and 4). Upon cross-linking with OSSC-6, the well-defined T_g of the non-cross-linked systems is preplaced by a very broad and undefined transition. This change in behavior may be reasonably attributed to the cross-linking of the isopropen units forned by the hydrolysis of OSSC-6, leading to greater rigidity of the resulting nanoparticle. For the less rigid DBDMS-cross-linked particles, the T_g of the polystyrene units is less affected, and thus a better defined glass transition is observed.

To evaluate the impact of the degree of internal cross-linking, static light-scattering experiments were performed for samples

dx.doi.org/10.1021/mz3006439 | *ACS Macro Lett.* 2013, 2, 121−124

obtained from the one-pot synthesis using the OSSC-6 cross-linker. Zimm plots were used to evaluate the weight-averaged molecular weight of the micelles and particles. Unfortunately, external cross-linking prevented evaluation of micelles obtained from the multi-step synthesis protocol. For the one-pot synthesis, photoinduced micellation without addition of a cross-linker leads to particles with an average radius of gyration r_g of 32 ± 3 nm and an average molecular weight M_w of 580 ± 50 kDa. A straightforward comparison of these values with those obtained from the P4^{t}BS-*b*-PS starting material (i.e., 22 ± 3 nm and 210 ± 30 kDa) indicates micelles consists of approximately three polymer chains.

Following cross-linking with 0.2 mmol of OSSC-6, the average molecular weight of the particles increases slightly to 610 ± 30 kDa. While an increase is expected, it should be noted that the measured values are not statistically different. Increasing the degree of cross-linking upon addition of 0.4 mmol of OSSC-6 leads to a substantial and significant increase of particle molecular weight to 1.2 ± 0.1 MDa.

In summary, we demonstrated a facile photoinduced synthesis of core cross-linked micelles via two different pathways in the presence of a photoacid generator. Regardless of the method employed, addition of the siloxane cross-linker consistently leads to shrinkage of the micelle hydrodynamic radii and changes in particle swelling behavior. To obtain well-defined nanoparticles, complete encapsulation of the PAG during micelle formation was found to be essential to suppress intermicellar cross-linking reactions. The favorable combination of synthetic simplicity together with the use of light as a stimulus make this approach an easy-to-use method for the generation of highly rigid core cross-linked micelles. If cyclic siloxane compounds are used, the formed siloxane core bears olefinic groups that allow postsynthetic modification.

■ ASSOCIATED CONTENT

Ⓢ Supporting Information

Additional experimental details. This material is available free of charge via the Internet at http://pubs.acs.org.

■ AUTHOR INFORMATION

Corresponding Author

*E-mail: rieger@tum.de.

Present Addresses

[†]Consortium für elektrochemische Industrie der Wacker Chemie AG Zielstattstraße 30, 81379 München, Germany.

[§]Professur für Makromolekulare Chemie, Department Chemie, Technische Universität Dresden, Zellescher Weg 19, 01069 Dresden, Germany.

[∥]Department of Chemistry, University of Alberta, Edmonton, Alberta, T6G 2G2, Canada; NRC-National Institute for Nanotechnology, Edmonton, Alberta, T6G 2M9, Canada.

Author Contributions

[⊥]Christian Anger, Frank Deubel, and Stephan Salzinger contributed equally.

Notes

The authors declare no competing financial interest.

■ ACKNOWLEDGMENTS

Funding from Consortium für elektrochemische Industrie der Wacker Chemie AG is acknowledged. Prof. Plank is thanked for the opportunity to measure dynamic light scattering.

■ REFERENCES

(1) Ahlheim, M.; Hallensleben, M. L. *Die Makromol. Chem.* **1992**, *193*, 779.
(2) Ishihara, M.; Nakanishi, K.; Ono, K.; Sato, M.; Kikuchi, M.; Saito, Y.; Yura, H.; Matsui, T.; Hattori, H.; Uenoyama, M.; Kurita, A. *Biomaterials* **2002**, *23*, 833.
(3) Li, Y. *Appl. Phys. Lett.* **1999**, *74*, 2233.
(4) Sideratou, Z.; Tsiourvas, D.; Paleos, C. M. *Langmuir* **1999**, *16*, 1766.
(5) Yoon, K. A.; Burgess, D. J. *J. Pharm. Pharmacol.* **1997**, *49*, 478.
(6) Lawrence, M. J.; Lawrence, S. M.; Barlow, D. J. *J. Pharm. Pharmacol.* **1997**, *49*, 594.
(7) Kawata, Y. *Appl. Phys. Lett.* **2006**, *88*, 123113.
(8) Chen, W.-J.; Li, G.-Z.; Zhou, G.-W.; Zhai, L.-M.; Li, Z.-M. *Chem. Phys. Lett.* **2003**, *374*, 482.
(9) Majhi, P. R.; Blume, A. *Langmuir* **2001**, *17*, 3844.
(10) Yoshida, E.; Ohta, M.; Terada, Y. *Polym. Adv. Technol.* **2005**, *16*, 183.
(11) Triolo, R. *Science* **1996**, *274*, 2049.
(12) Zhou, S.; Chu, B. *Macromolecules* **1998**, *31*, 5300.
(13) Yoshida, E.; Kuwayama, S.; Kawaguchi, S. *Colloid Polym. Sci.* **2010**, *288*, 91.
(14) Jiang, J.; Qi, B.; Lepage, M.; Zhao, Y. *Macromolecules* **2007**, *40*, 790.
(15) Leclair, S.; Mathew, L.; Giguère, M.; Motallebi, S.; Zhao, Y. *Macromolecules* **2003**, *36*, 9024.
(16) Saji, T.; Hoshino, K.; Aoyagui, S. *J. Am. Chem. Soc.* **1985**, *107*, 6865.
(17) Saji, T.; Ebata, K.; Sugawara, K.; Liu, S.; Kobayashi, K. *J. Am. Chem. Soc.* **1994**, *116*, 6053.
(18) Yoshida, E.; Tanaka, T. *Colloid Polym. Sci.* **2006**, *285*, 135.
(19) Szczubiałka, K.; Nowakowska, M. *Polymer* **2003**, *44*, 5269.
(20) Matějka, L.; Dušek, K. *Die Makromol. Chem.* **1981**, *182*, 3223.
(21) Pieroni, O.; Fissi, A. *J. Photochem. Photobiol. B: Biol.* **1992**, *12*, 125.
(22) Menju, A.; Hayashi, K.; Irie, M. *Macromolecules* **1981**, *14*, 755.
(23) Taguchi, M.; Li, G.; Gu, Z.; Sato, O.; Einaga, Y. *Chem. Mater.* **2003**, *15*, 4756.
(24) Meier, H. *Angew. Chem., Int. Ed. Engl.* **1992**, *31*, 1399.
(25) Eastoe, J.; Dominguez, M. S.; Wyatt, P.; Beeby, A.; Heenan, R. K. *Langmuir* **2002**, *18*, 7837.
(26) Irie, M.; Hosoda, M. *Makromol. Chem., Rapid Commun.* **1985**, *6*, 533.
(27) Dunkin, I. R.; Gittinger, A.; Sherrington, D. C.; Whittaker, P.; Whittaker, P. *J. Chem. Soc., Chem. Commun.* **1994**, 2245.
(28) Mezger, T.; Nuyken, O.; Meindl, K.; Wokaun, A. *Prog. Org. Coat.* **1996**, *29*, 147.
(29) Nuyken, O.; Voit, B. *Macromol. Chem. Phys.* **1997**, *198*, 2337.
(30) Veronese, A.; Berclaz, N.; Luisi, P. L. *J. Phys. Chem. B* **1998**, *102*, 7078.
(31) Conlon, D. A.; Crivello, J. V.; Lee, J. L.; O'Brien, M. J. *Macromolecules* **1989**, *22*, 509.
(32) Yoshida, E.; Kuwayama, S. *Colloid Polym. Sci.* **2008**, *286*, 1621.
(33) Kataoka, K.; Harada, A.; Nagasaki, Y. *Adv. Drug Delivery Rev.* **2001**, *47*, 113.
(34) Davis, M. E.; Chen, Z. G.; Shin, D. M. *Nat. Rev. Drug Discovery* **2008**, *7*, 771.
(35) Kabanov, A.; Batrakova, E.; Sherman, S.; Alakhov, V. *Adv. Polym. Sci.* **2006**, 173.
(36) Torchilin, V. P. *J. Controlled Release* **2001**, *73*, 137.
(37) Wooley, K. L. *J. Polym. Sci., Part A: Polym. Chem.* **2000**, *38*, 1397.
(38) Anger, C. A.; Hindelang, K.; Helbich, T.; Halbach, T.; Stohrer, J.; Rieger, B. *ACS Macro Lett.* **2012**, *1*, 1204.